Science Advances
AAAS

advances.sciencemag.org/cgi/content/full/6/47/eabb7232/DC1

Supplementary Materials for

Amazon rainforest photosynthesis increases in response to atmospheric dryness

J. K. Green*, J. Berry, P. Ciais, Y. Zhang, P. Gentine

*Corresponding author. Email: julia.green@lsce.ipsl.fr

Published 20 November 2020, *Sci. Adv.* **6**, eabb7232 (2020)
DOI: 10.1126/sciadv.abb7232

This PDF file includes:

Table S1. CMIP5 Model Information.

Modeling Center (or group)	Institute ID	Model Name
Beijing Climate Center, China Meteorological Administration	BCC	BCC-CSM1-1
Canadian Centre for Climate Modelling and Analysis	CCCMA	CanESM2
National Center for Atmospheric Research/ University Corporation for Atmospheric Research	NCAR/UCAR	CCSM4
National Center for Atmospheric Research/ University Corporation for Atmospheric Research	NCAR/UCAR	CESM1-BGC
NOAA Geophysical Fluid Dynamics Laboratory	NOAA GFDL	GFDL-ESM2M
Institute of Numerical Mathematics, Russian Academy of Sciences	INM RAS	INM-CM4
Institut Pierre-Simon Laplace	IPSL	IPSL-CM5A-LR
Japan Agency for Marine-Earth Science and Technology (JAMSTEC), Centre for Climate System Research / National Institute for Environmental Studies, Japan.	MIROC	MIROC-ESM
Meteorological Research Institute (MRI) of Japan	MRI	MRI-ESM1
Norwegian Climate Center	NCC	NorESM1-M

Table S2. Flux tower information

Site ID	Site Description	Data availability
Manaus-ZF2 K34/ BR-Ma2	Wet, tropical rainforest	January 2002-December 2004
Santarem-Km67-Primary Forest/BR-Sa	Wet, tropical rainforest	January 2002-December 2004
Tocantins – Ilha do Bananal/BR-BAN	Seasonally flooded forest, savannah and grassland	January 2004-December 2006

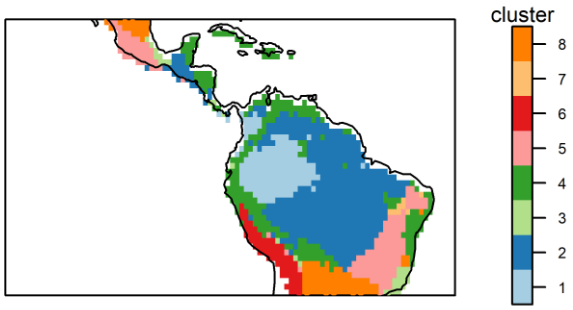

Fig. S1. K-means clustering results. The clusters generated via a k-means clustering analysis using precipitation, radiation, temperature, VPD, and SIF data as inputs. Monthly data is used from the time period of 2007-2016. Clusters are ranked from wettest (cluster 1) to driest (cluster 8).

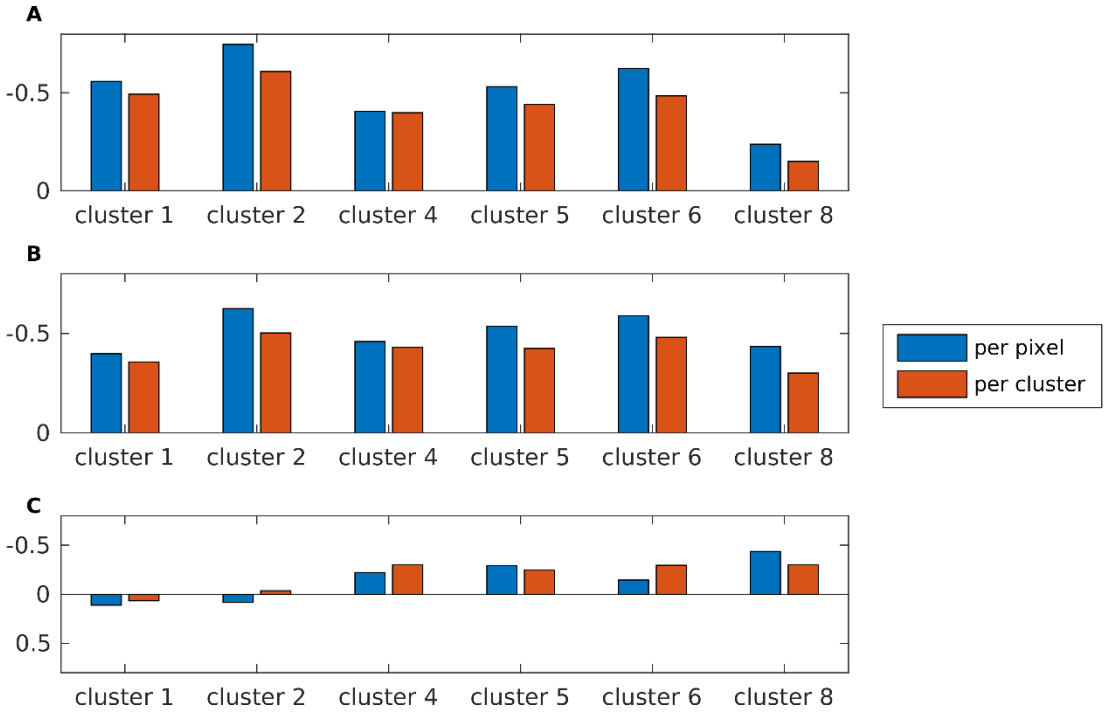

Fig. S2. VPD and precipitation correlations. Correlations between VPD and precipitation at a 0-month lag (**A**), a 2-month lag (**B**), and a 4-month lag (**C**). The median correlation between VPD and precipitation for each pixel within a cluster is depicted in blue, while the correlation of VPD and precipitation using all pixels per cluster is displayed in orange.

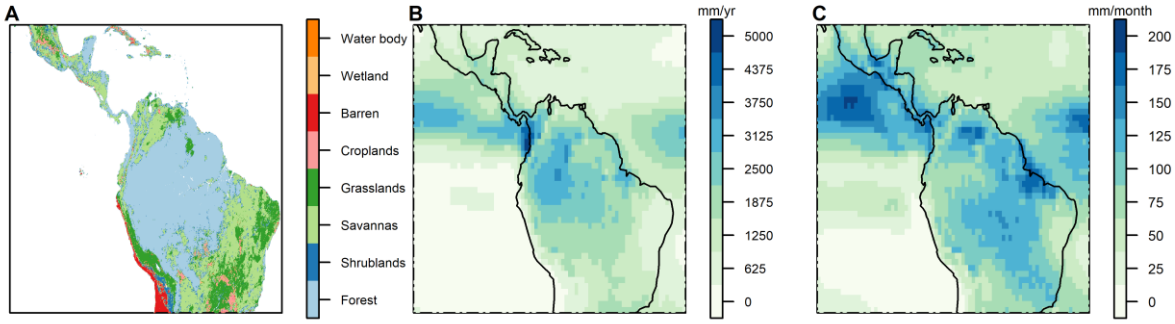

Fig. S3. Land cover types and precipitation. Land cover types from MODIS land cover data (**A**), average precipitation per year (**B**), and the standard deviation of the monthly GPCP precipitation data (2007-2016) (**C**) in the tropical region of the Americas.

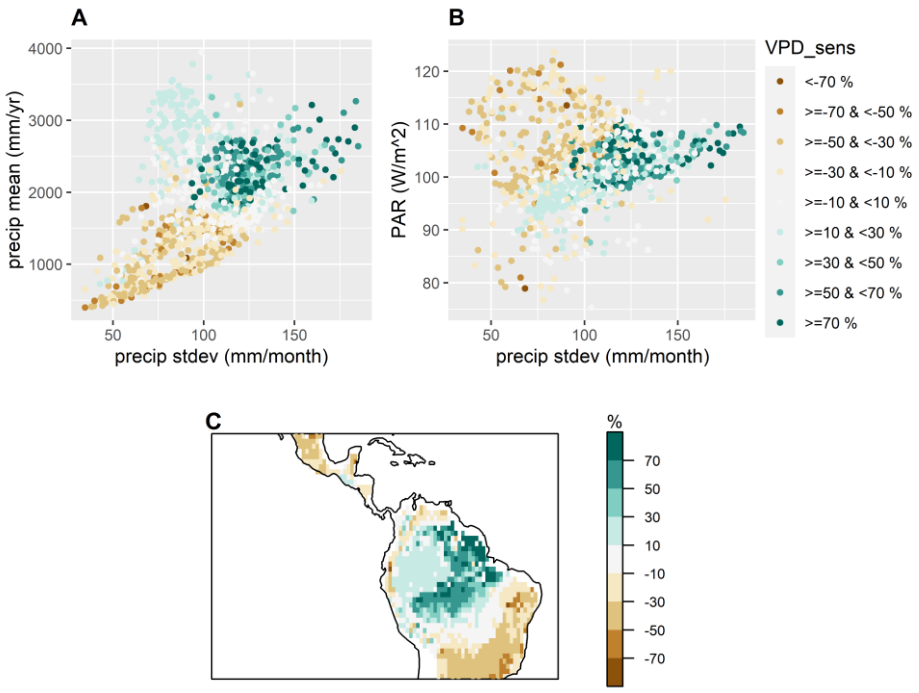

Fig. S4. VPD sensitivity scatter plots: full year. Mean annual precipitation vs. the standard deviation of precipitation (**A**), and mean PAR vs. the standard deviation of precipitation (**B**) for each pixel location within the study area. The color of each point corresponds to that location's SIF sensitivity to VPD for the full year (dry and wet season together) (**C**), as determined by the artificial neural network analysis.

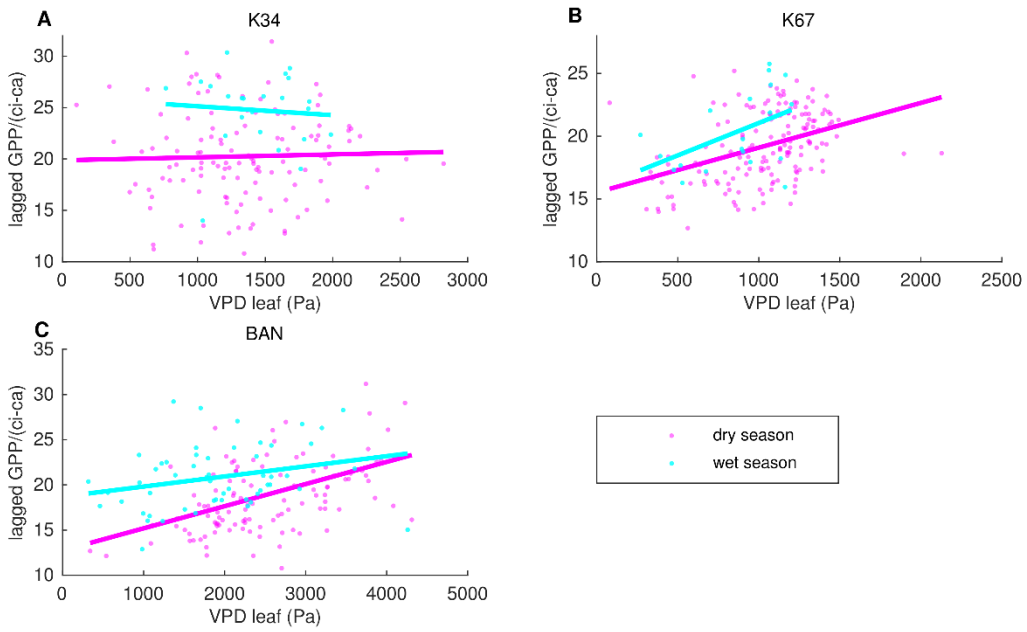

Fig. S5. Lagged biogeochemistry flux tower results vs. VPD. Flux tower data from three sites (K34 (**A**), K67 (**B**) and BAN (**C**)) in Amazonia showing the mean climatology of GPP normalized by the ratio of leaf internal CO_2 partial pressure (c_i) to atmospheric CO_2 partial pressure (c_a) lagged by two months versus VPD at the leaf surface. Daytime data with no precipitation is used for varying time periods between 2002 and 2006 based on data availability.

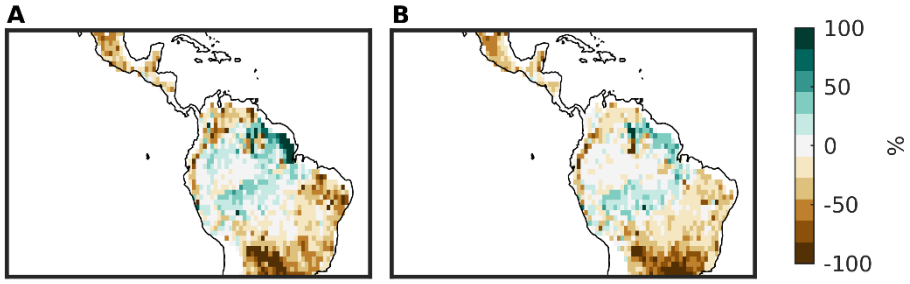

Fig. S6. ANN sensitivity analysis results for an extreme event. Remote sensing results for the dry season sensitivity of SIF to VPD for a non-anomalous year, 2014 (**A**), and of dry season sensitivity of SIF to VPD for the 2015 El Niño (**B**).

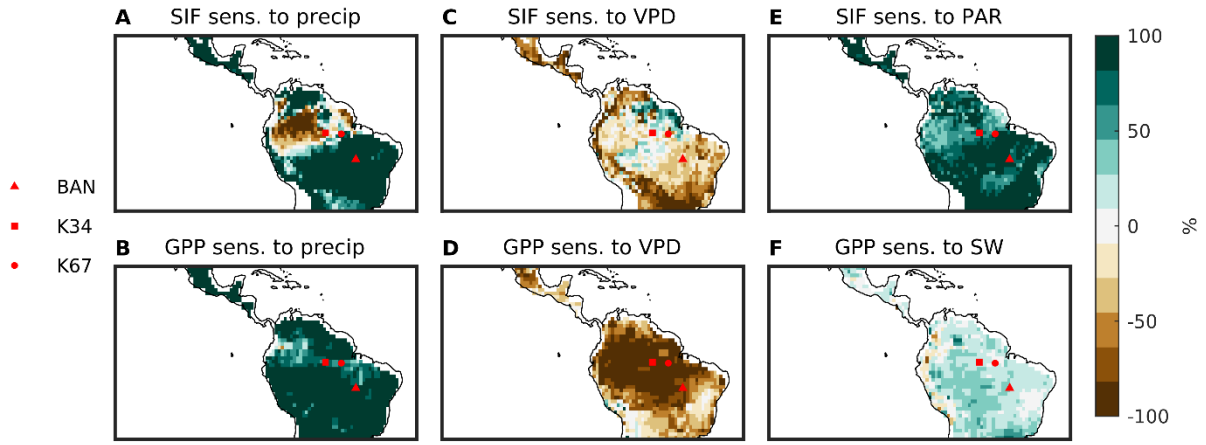

Fig. S7. ANN sensitivity analysis results using 2 standard deviations: dry season. Remote sensing results for the sensitivity of SIF to precipitation (**A**), VPD (**C**), and PAR (**E**). Stippling represents areas of a median r-value > 0.6. Model results for the sensitivity of GPP to precipitation (**B**), VPD (**D**), and SW (**F**). Stippling represents regions where at least 6 of the 10 models agree on the sign of the feedback depicted.

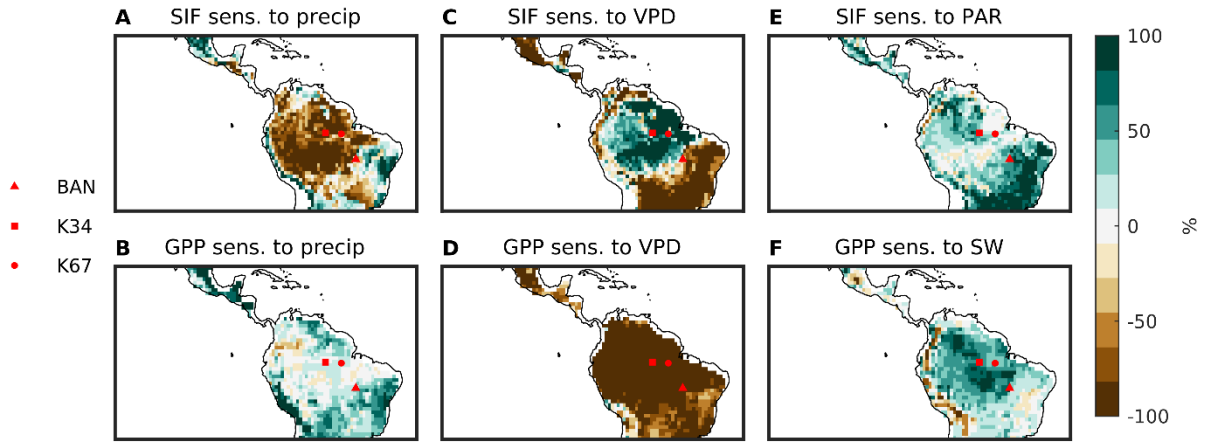

Fig. S8. ANN sensitivity analysis results using 2 standard deviations: wet season. Remote sensing results for the sensitivity of SIF to precipitation (**A**), VPD (**C**), and PAR (**E**). Stippling represents areas of a median r-value > 0.6. Model results for the sensitivity of GPP to precipitation (**B**), VPD (**D**), and SW (**F**). Stippling represents regions where at least 6 of the 10 models agree on the sign of the feedback depicted.

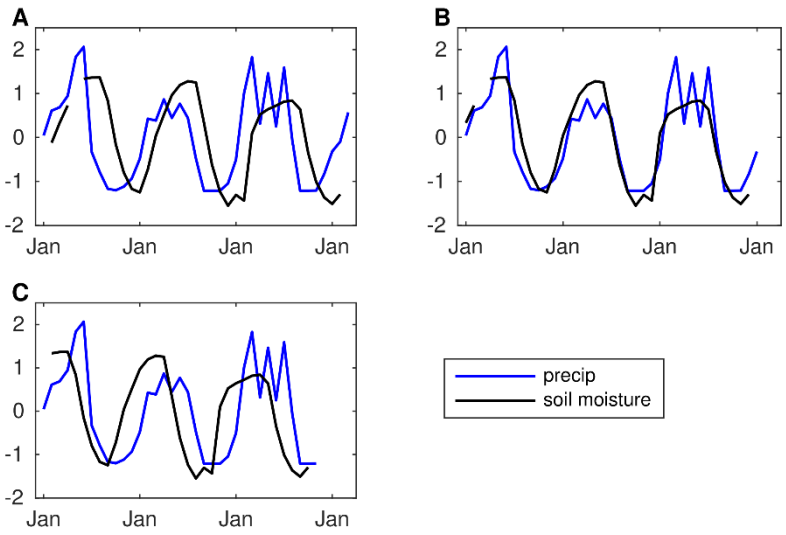

Fig. S9. Soil moisture and precipitation time series. The time series of monthly soil moisture and precipitation flux tower data normalized by their means and standard deviations for BAN at a 0-month lag (**A**), soil moisture with a 2-month lag (**B**), and soil moisture with a 4-month lag (**C**). BAN is the only tower used for this analysis as it is the only tower with publicly available soil moisture data.